

Characteristics of pack ice stress in the Alaskan Beaufort Sea

J. A. Richter-Menge and B. C. Elder

Cold Regions Research and Engineering Laboratory, Hanover, New Hampshire

Abstract. Ice stresses in a multiyear floe were continuously monitored over 6 months in the fall-winter-spring of 1993–1994. Stresses sensors were installed at sites near the edge and at the center of the floe, which was located in the pack ice of the Alaskan Beaufort Sea. Compressive stresses in the major principal stress component varied significantly among the measurement sites, being of greater magnitude and exhibiting more high-frequency variations at the edge than at the center of the floe. Maximum compressive stresses, measured at a site 400 m from the edge of the floe, ranged from 100 to 300 kPa. Tensile stresses (maximum of 50 kPa) and the minor principal stress component (± 50 kPa) were relatively constant at all measurement sites. A cross-correlation analysis indicates that the minor principal stress is strongly correlated to changes in the ice temperature. This result suggests that the minor principal stress component provides a good first-order approximation of thermally induced stresses. Correlation between the major principal stress component and the ice temperature at the center site was also high, but weakened near the edges of the floe where the ice-motion-induced stresses became more significant. Attempts to filter the major principal stress signal to separate the thermal and ice-motion-induced stresses were unsuccessful. This result implies that the ice-motion-induced stresses, distinguished by variations in magnitude of the order of hours, also have a significant low-frequency content similar to the thermal stresses. These low-frequency changes occur over a period of days. Seasonal variations in the characteristics of the stress were also evident and are likely to reflect the developing continuity of the pack as the winter season progresses.

1. Introduction

The internal ice stress generated by ice motion is a fundamental term in the momentum balance equation used to govern ice dynamics models. A widely applied ice dynamics model for the Arctic basin was developed by Hibler [1979]. In this model and derivatives of it [e.g., Semtner, 1987; Oberhuber, 1993; Pollard and Thompson, 1994; Weatherly et al., 1997] the ice is represented by a viscous-plastic rheology that relates the internal ice stress to deformation. Deformation is, in turn, dependent on an empirically defined ice strength, which is a function of the ice concentration and thickness. The ice strength is chosen by comparing model predictions of ice concentration and drift to data collected from drifting buoys, satellite imagery, and submarine-based ice thickness profiles. For basin-scale models this comparison suggests that the compressive strength of the ice is of the order of 1–10 kN m^{-1} [Thorndike et al., 1975; Hibler, 1979]. It is typically assumed that this maximum compressive strength is a reflection of the forces associated with ridge building in the ice pack [Rothrock, 1975; Hibler, 1980; Hopkins, 1996].

Direct measurements of pack ice stress have been made in several studies. Comfort et al. [1994] report the results of a series of field experiments, held during spring 1986, 1989, and 1991, where stress sensors were installed in the center of multiyear ice floes in the southern Beaufort Sea. Applying a finite element model, it was estimated that stresses at the edge of the floes, assumed to be indicative of ridge-building forces, ranged from 24 to 1191 kN m^{-1} during these experiments. Coon et al.

[1989] and Tucker and Perovich [1992] measured ice stresses in drifting pack ice in the eastern Arctic for 2 months during fall 1988. Their results suggest that ridge-building forces were 37 and 100–200 kN m^{-1} , respectively. Nikitin and Kolesov [1993] summarized calculated ridging forces for a variety of ice types. These forces ranged from 150 kN m^{-1} for 0.30-m-thick young ice to 1720 kN m^{-1} for second-year ice that is 2.5 m thick. Combined, these investigations indicate that ridge-building forces estimated from stress measurements are an order of magnitude larger than the ice strength derived from ice dynamics models.

The overall goal of our work is to improve the understanding of the relationship between the modeled and measured estimates of ice strength. Once this relationship is established, measurements of ice stress and deformation can be appropriately used for a direct, rather than implicit, evaluation of ice dynamics models. The internal ice stress term in the momentum balance equation of an ice dynamics model represents the globally averaged pack ice stress, which is not the same as the ice stress that occurs at a point of local failure at a boundary. Intuitively, it would seem that the stresses at the center of a multiyear floe would be the most comparable, since they presumably represent the integration of all the edge stresses. This, in fact, has been the working hypothesis for a number of ice stress investigations, but it has never been thoroughly tested [Croasdale et al., 1988].

To specifically investigate the distribution of stress in a multiyear floe, we installed stress sensors at the center and edge of a floe in the pack ice of the Alaskan Beaufort Sea. These sensors were continuously monitored for 6 months, from October 1993 through March 1994. In this paper we present an analysis of the ice stress measurements, focusing on a compar-

This paper is not subject to U.S. copyright. Published in 1998 by the American Geophysical Union.

Paper number 98JC01261.

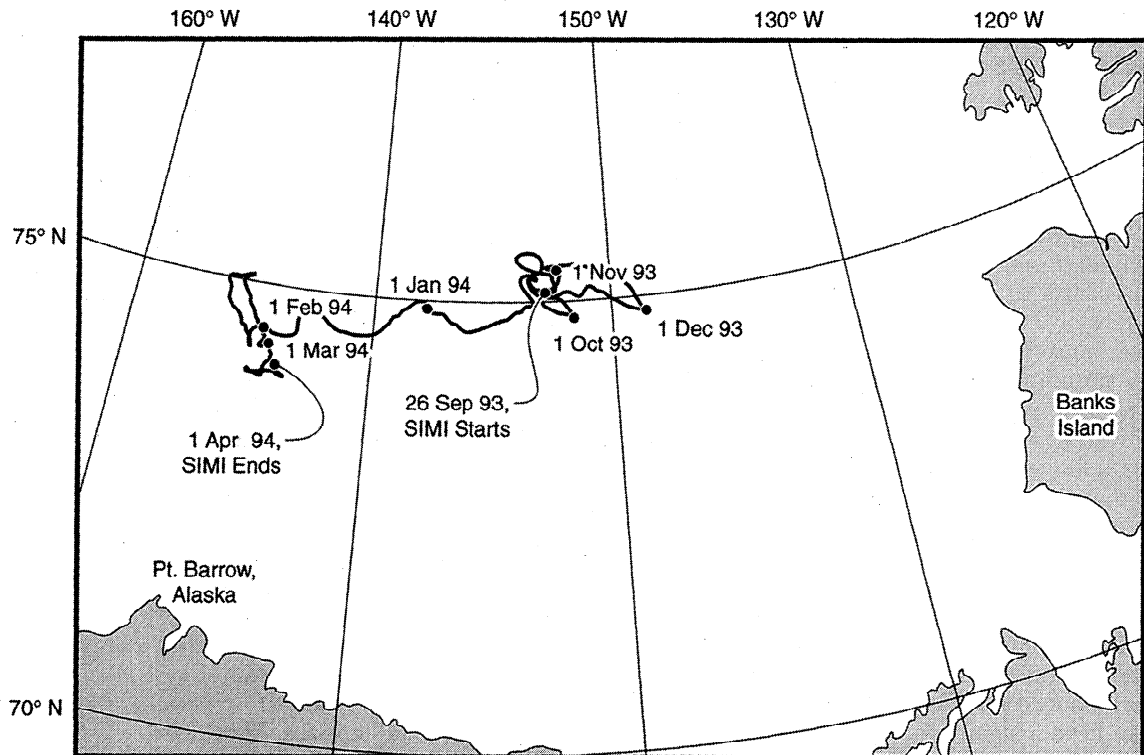


Figure 1. Drift track of the multiyear floe that served as a base camp for the Sea Ice Mechanics Initiative (SIMI).

ison of the stress time series from the sensors located on the multiyear floe. The results of a cross-correlation analysis between ice temperature and ice stress and of an effort to apply signal-filtering techniques to separate thermally and motion-induced stress are discussed to more clearly establish the origins of the stress. The process of stress transmission through the pack and its seasonal dependence are also addressed.

2. Field Measurement Program

Our work was done as part of the U.S. Office of Naval Research's 5-year accelerated research initiative, Sea Ice Mechanics Initiative (SIMI), which began in October 1991. This program supported field, laboratory, computer, and theoretical studies to explore the relationship of the mechanical behavior of sea ice observed at various scales, ranging from 10^{-2} to 10^5 m. Of specific interest was the possible application of laboratory results in the description of geophysical-scale ice failure processes.

The main field program of SIMI was held over the fall-winter-spring season of 1993–1994. In late September 1993 the U.S. Coast Guard icebreaker *Polar Star* was used to establish a base camp at the edge of the pack ice in the Alaskan Beaufort Sea. The site chosen for the camp was a multiyear floe approximately 450 km north of the Alaskan coast (75°N , 142°W) (Figure 1). The multiyear floe was roughly 2 km in diameter and had an average ice thickness of 1.44 m in mid-November. The most distinguishing feature of this floe was a significant area of level, first-year ice, approximately 200 m wide and extending 1500 m from the edge toward the center of the floe. There were no pronounced ridge sails in the floe.

The camp was occupied from late September until early December and from early March through early April. One

brief visit was made to the camp in mid-February to evaluate its condition. When the camp was abandoned in early April 1994, the floe had drifted approximately 250 km to the west (74°N , 155°W). As shown in Figure 1, most of this movement occurred during December and January. The total rotation of the floe over the course of the experiment was estimated to be 60° , clockwise. While no one occupied the camp between December and March, our equipment was designed to run autonomously. This allowed data collection to continue uninterrupted through the entire experiment.

2.1. Stress Sensor

Central to our investigation was the collection of high-quality, in situ measurements of ice stress. These were made using the cylindrical, vibrating wire sensors described by *Johnson and Cox* [1982]. These sensors have undergone extensive laboratory tests to determine their reliability [*Cox and Johnson*, 1983] and have been successfully used in other Arctic field programs [*Johnson et al.*, 1985; *Tucker and Perovich*, 1992]. Each sensor provides information on the stress acting at a point in the horizontal plane of the ice cover. Stresses are determined by measuring changes in the radial deformation of a cylindrical steel annulus, using a 120° , three-wire rosette. The wires in the rosette stretch across the hollow center of the annulus at the midpoint along its length. Changes in the diameter of the annulus cause a change in the frequency of vibration of each wire, which are plucked magnetically. Knowing the material properties of the steel annulus, this change in frequency can be directly related to the stress applied to the sensor.

The laboratory tests done by *Cox and Johnson* [1983] to evaluate this stress sensor design involved embedding the sensor in both fresh and saline ice blocks and loading the ice

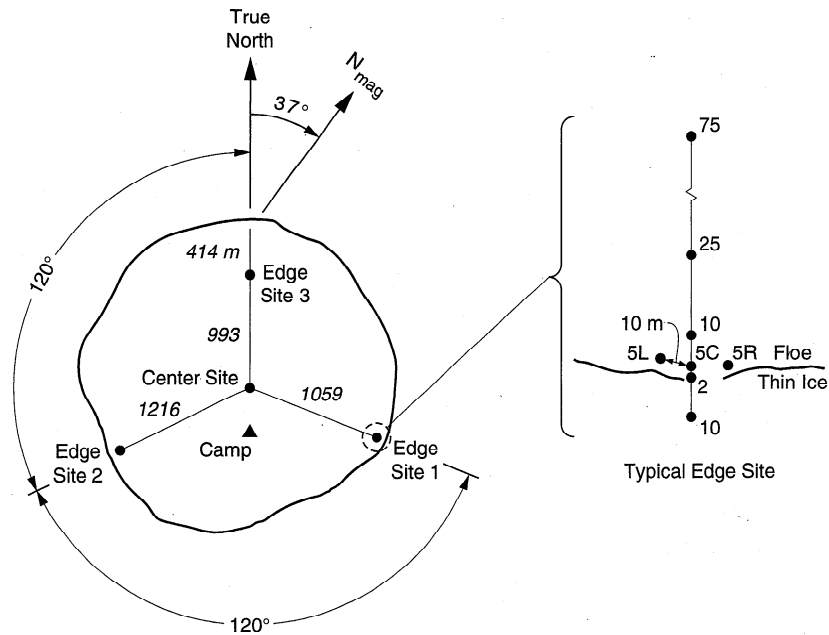


Figure 2. Locations of stress sensors on the instrumented multiyear floe. All of the sensors were placed near the surface of the ice, an average of 22.1 cm below the ice surface, with the exception of the site at the center of the floe where sensors were also located at depths of 1.0 and 2.0 m.

blocks in a biaxial load frame. The results indicated that over a loading range of 0 to 2 MPa the measured stress was within 15% of the applied stress and the stress direction was typically correct to within 5°. The tests also established that the resolution of the stress sensor was 20 kPa. Temperature sensitivity tests showed that stresses vary linearly with temperature at a rate of about 5 kPa °C⁻¹. To allow corrections for the temperature effect to be made to the data, each sensor is equipped with a thermistor. This thermistor also provides a measurement of the ice temperature at the sensor at the time of the stress measurement.

Calibration tests to determine the specific relationship between the diametral deformation and the vibration frequency of each wire in each stress sensor, each wire's temperature sensitivity, and the reading of each wire at 0 kPa, 0°C are required before field use. For this investigation each sensor was calibrated by placing it in an air-filled pneumatic sleeve that applied a uniform, hydrostatic pressure. The sleeve was located in a temperature-controlled environmental chamber, which was held constant at 0, -10°C, or -20°C. At each of these temperatures, readings from each wire of the sensor were taken at applied stresses of 0, 250, and 500 kPa. The stress was ramped upward and then downward during the course of the calibrations.

The most critical calibration measurement in the stress analysis is the response of the wires at 0 kPa, 0°C. It has also proven to be the most sensitive, changing during shipment and installation and exhibiting a linear drift during the course of an experiment. To define any changes in this calibration term during shipping, sensor readings were taken in an ice bath once we arrived in the field. After the sensor was frozen into the ice cover, the output at 0 kPa was again determined during a period when there was no ice motion and no significant temperature change. Since the temperature of the sensor during this reading was below 0°C, the reading had to be adjusted to 0°C using the laboratory results on temperature sensitivity. A

final calibration was made at the end of the experiment by cutting a block of ice around the sensor and freeing it from the sheet. The in-ice calibrations proved to be the most useful. The 0 kPa, 0°C reading applied in our analysis was defined by using the in-ice determinations at the beginning and end of the experiment and assuming that any variation over the period was linear.

2.2. Sensor Array

Sensors on the central multiyear floe were deployed in an array designed to investigate the horizontal spatial distribution of stresses in a floe. Of particular interest was a comparison of stresses measured at the center and edge of the floe to better understand the process of stress transmission through the ice pack. In previous studies, stresses have been measured at the center of the floe [Comfort and Ritch, 1990; Comfort et al., 1992], at the edge of the floe [Tucker and Perovich, 1992], or near a site of active ridging [Coon et al., 1989]. The relationship between the stresses at these different locations has only been inferred through the use of finite element models [Frederking and Evgin, 1990].

Our experimental plan was to collect concurrent measurements of stress at one center and three edge sites on the floe (Figure 2). The edge sites initially were located at 120° intervals around the perimeter of the floe, with edge site 3 at the northern point. The perimeter was defined by the presence of open water at the time of deployment. This definition of "the floe" resulted in the inclusion of two significant areas of first-year ice. At edge site 3 there was a large pan of young first-year ice that had developed along the edge of the multiyear ice. Edge site 1 lay just below the 1500 m × 20 m area of first-year ice that extended from the edge toward the center of the floe. A total of seven sensors were deployed in the multiyear ice at each of the edge sites. Five of these sensors were positioned along a line that extended from the edge to the center of the floe. They were located at 2, 5, 10, 25, and 75 m from the edge.

Table 1. Summary of Stress Sensors Used

Sensor	Distance From Edge, m	Ice thickness on About October 1, m	Wire Depth Below Surface, m
<i>Edge Site 1</i>			
E1-2	2	1.73	0.44
E1-5R	5	1.22	0.25
E1-10	10	0.32	0.22
E1-75	75	0.31	0.20
<i>Edge Site 3</i>			
E3-402	402	0.85	0.23
E3-405C	405	0.27	0.21
E3-405L	405	0.80	0.21
E3-410	410	0.99	0.20
E3-425	425	0.28	0.26
<i>Center Site</i>			
C1-T	≈1200	2.13	0.38
C1-M			0.98

All sensors operated from October 7, 1993, through March 21, 1994. Sensor identification numbers (E1-2) indicate the site where the sensor was located (edge site 1), the distance from the edge of the floe (2 m), and, if applicable, whether the sensor was to the right (R), left (L), or along (C) the line running toward the center of the floe (Figure 2). At center site the location of the sensor near the top (T) or middle (M) of the ice cover is indicated.

At the 5-m position, two sensors were placed 10 m to the left and right of the line. This edge layout was chosen to provide information on the amount of stress attenuation over a short distance near the edge of the floe and on the distribution of stress along the boundary. This experimental plan was followed in our initial deployment, which took place from September 24 to 28, 1993. It was necessary, however, to abandon edge site 2 and relocate edge site 3 400 m back from the edge of the floe owing to significant deformation events early in the experiment. At the center of the floe, one sensor was located 38 cm below the ice surface in late September. A thermistor string, extending above and below the ice surface, was also installed at this site [Perovich *et al.*, 1997]. On November 29, 1993, two more sensors were located at the center site at depths of 1 and 2 m below the ice surface. Analysis of the data from this site indicated that the 2-m sensor did not provide any reliable stress measurements.

The sensors were removed from the ice between March 17 and 24, 1994. During the course of the experiment, several of the cables that connected the stress sensors to the data loggers were damaged by foxes, ending the stress time series at that sensor site. Measurements from these sites were not used in the current analysis. A summary of the sensors used in the analysis presented in this paper and their location on the multi-year floe is given in Table 1.

The sensors were installed in a 10-cm-diameter hole drilled in the ice using standard coring equipment. A PVC pipe was attached to the end of the sensor so that it could be located downhole. The sensor was suspended at the desired depth by placing a crossbar, which rested on the ice surface, through the PVC pipe extension. All of the sensors in this experiment were located at approximately the same horizontal level in the ice sheet, with the wire rosette an average of 22.1 cm below the ice surface. Once the sensor was properly located, it was frozen into the ice cover. In the fall, when the ice was relatively warm and porous, this was accomplished by drilling the hole through the thickness of the ice cover so that it would backfill with

seawater. Later in the program, holes could be filled by pouring freshwater into them. Our records indicated that the compressive stresses associated with freeze-in were typically 100 kPa and took 2–4 days to dissipate. Tucker and Perovich [1992] reported similar observations when installing the same sensor for their program. Synchronized readings from all of the sensors were made throughout the experiment at 5-min intervals.

A survey of the snow and ice thickness distribution along the legs extending from each edge site to the center of the floe was made in mid-November 1993. Ice thickness was determined by drilling a hole through the ice cover. In the vicinity of the edge sites, thickness was measured every 5 m and next to every sensor location. After reaching a point 100 m from the stress sensor closest to the edge, thickness was measured every 50 m. The results of this survey in the vicinity of edge sites 1 and 3 are presented in Figure 3. In total we made 137 thickness measurements in the floe during this survey. The mean ice thickness was 1.44 ± 0.85 m, with a range of 0.39 to >4.00 m.

3. Results and Discussion

In this presentation of results the sign convention is positive for compressive stress.

3.1. Spatial Variability

The time series for major (σ_1) and minor (σ_2) principal stresses measured at edge sites 1 and 3 and center site are presented in Figure 4. For this comparison the sensors closest to the edge of the floe were chosen from the edge sites. At edge site 1 the sensor was 2 m from the edge, and at edge site 3 it was 400 m from the edge. All three records give near-surface stresses. The depths below the ice surface of the wire rosette in the sensors at center site, edge site 1, and edge site 3 were 0.38, 0.44, and 0.20 m, respectively. The time series extend from October 7, 1993, to March 21, 1994.

Significant spatial variability in the characteristics of the stress over the region of the floe is readily apparent. A primary attribute of the stress time series is that the major and minor principal stresses at all three sites have both a low-frequency (of the order of days) and high-frequency (of the order of hours) content. Variations in the relative magnitude of the high-frequency content in the major principal stress component constitute the most pronounced difference in the characteristics of the stress signature between these sites. At edge site 3 (Figure 4a) the high-frequency content in σ_1 is persistent and often dominant. Peak compressive stresses during periods of significant high-frequency activity typically ranged from 100 to 200 kPa, reaching a maximum of 300 kPa on November 30. At edge site 1 (Figure 4b) the high-frequency content in σ_1 is still persistent, with periods of significant activity corresponding temporally to those observed at edge site 3. However, the peak compressive stress during these events was generally lower at edge site 1 compared with edge site 3. Peak stresses varied between 50 and 100 kPa, about one third of the magnitude measured at edge site 3. It is interesting that the site 400 m in from the edge of the floe experienced higher stress than the site 2 m from the edge. This demonstrates the complex process of stress distribution in a multiyear floe. The distribution of stress is dependent on the location of points of load transmission to the floe, the boundary conditions at the points of transmission, and ice thickness variations in the floe. Low-frequency changes dominate the major principal stress at center site. During periods of significant high-frequency activity at

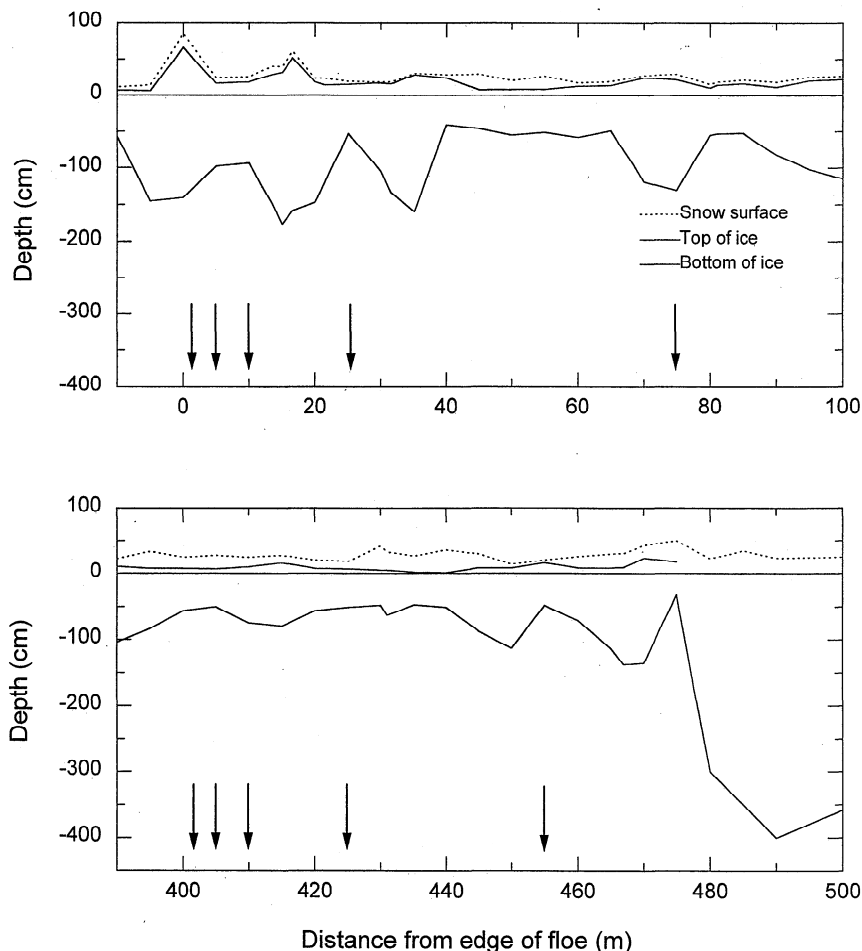


Figure 3. Ice and snow thickness distribution at stress sensor edge sites (top) 1 and (bottom) 3, located near the edge of the multiyear floe. Arrows indicate the location of the stress sensors.

the edge sites, high-frequency changes in σ_1 at the center of the floe were typically less than 20 kPa. In general, the compressive stress at center site remained relatively low, rarely exceeding 50 kPa. Compressive stresses greater than 100 kPa were recorded only once at center site during a low-frequency event on February 5. This event corresponded to an increase in air temperature of approximately 30°C (Figure 4d). This was the most significant air temperature increase during the winter period. The largest high-frequency peak at center site occurred on February 23 and represented a total change in stress of about 100 kPa, with a high-frequency contribution of about 50 kPa. Visual observations of the floe in early March indicated that a large crack ran through the center of the floe, within several hundred meters of center site, at about this time.

The peak compressive stress magnitudes at the various sites agree well with those reported by other investigators measuring stresses in pack ice environments. Monitoring the stress at the center of several multiyear floes, *Comfort et al.* [1992] measured variations in the maximum principal stress of between 5 and 10 kPa during periods when ice deformation was known to occur. A significantly larger stress variation of 290 kPa was reached once when a ridge-building event took place 95 m away from a sensor. *Tucker and Perovich* [1992] measured peak stresses of 180 kPa on a multiyear floe at a site 200 m from the edge, where a sensor was located 0.25 m below the ice surface. These peak stresses occurred during what are de-

scribed as extreme deformation events. *Coon et al.* [1989] reported a maximum average stress of 35 kPa during a ridging event located several hundred meters from the stress sensor.

The relative magnitude of the peak compressive stress between the edge sites during periods of significant high-frequency activity remained nearly consistent through the experiment, with σ_1 at edge site 3 $>$ σ_1 at edge site 1. The direction of the major principal stress at the edge sites was also fairly consistent during the periods of significant high-frequency stress activity (Figures 5a and 5b). The major principal stress direction at edge site 1 was in the NE and SW quadrant, ranging from N30°E (S30°W) to N60°E (S60°W) during most events, for example, November 26 to December 15, January 22–30, January 30 to February 4, and March 8–12 (Figure 5a). At edge site 3 during these same periods the major principal stress direction was in the NW and SE quadrant, varying from N60°W (S60°E) to west (east) (Figure 5b). One notable exception was the event from December 14 to January 2 when the direction of σ_1 at edge site 1 and edge site 3 was more northerly, at N20°W (S20°E) and north (south), respectively. This event is also exceptional in that the magnitude of the stresses at the two edge sites was more comparable (Figure 4). The difference in the direction of the principal stresses at the edge sites adds further evidence regarding the complexity of stress distribution in the multiyear floe.

Consistency in the relative magnitude of peak stresses be-

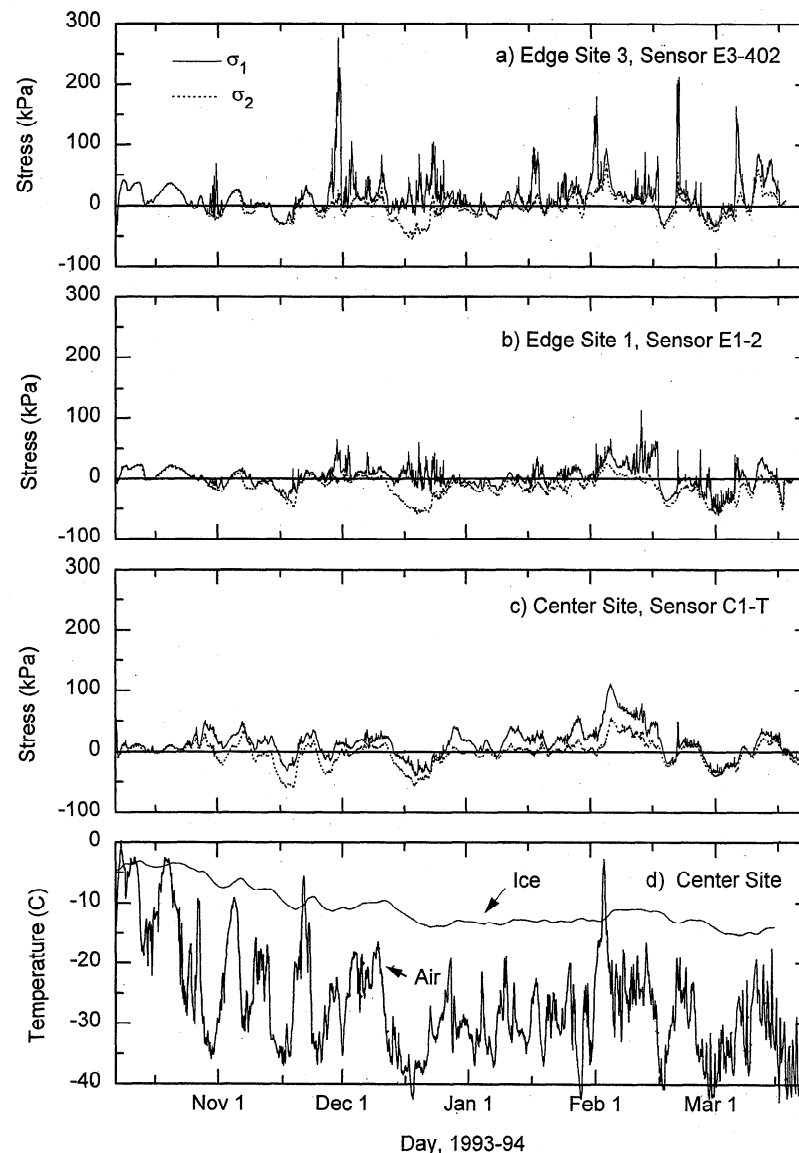


Figure 4. Time histories of the major σ_1 and minor σ_2 principal stress components at (a) edge site 3, (b) edge site 1, and (c) center site, and (d) the ice and air temperature at the center site, from October 7, 1993 to March 21, 1994.

tween the edge sites, in the temporal correspondence of the occurrence of these events, and in the direction of the principal stress during each event combine to suggest that the characteristics of the applied loads and boundary conditions affecting the instrumented floe did not vary substantially during this experiment. The observation of a repeated loading condition corresponds to the relatively set weather pattern that develops during the winter season and provides the atmospheric forcing for the system. The observation that the floe rotated a total of only 60° clockwise during the experiment supports the observation that the boundary conditions remained relatively stable throughout the winter.

It is evident in Figure 4 that there was little spatial variability among the three sites with respect to the minor principal stress. At all sites the minor principal stress was dominated by low-frequency variations, which typically ranged between plus and minus 50 kPa. An analysis of the linear relationship of the major and minor principal stress components between the

edge sites over the entire experiment demonstrates the difference in the degree of spatial variability between these components (Table 2). The correlation coefficients for σ_1 among the sites varies from 0.59 to 0.24. The correlation coefficient for σ_2 among the sites is consistently higher, ranging from 0.80 to 0.64. This result suggests that the minor principal stress originates from a source that also exhibits relatively little spatial variability.

Tensile stresses were common in both the major and minor principal stress components and also showed little spatial variability. The maximum tensile stress in the major principal component was consistently near 50 kPa. This finding is similar to the observations made by *Tucker and Perovich* [1992]. This tensile stress is far lower than the tensile failure strength of first-year sea ice, measured in the laboratory on small (≈ 10 cm) samples. The laboratory tests indicate a failure stress ranging from 200 to 800 kPa, depending on the ice temperature and its salinity [*Dykins*, 1970; *Kuehn et al.*, 1990; *Richter-Menge and*

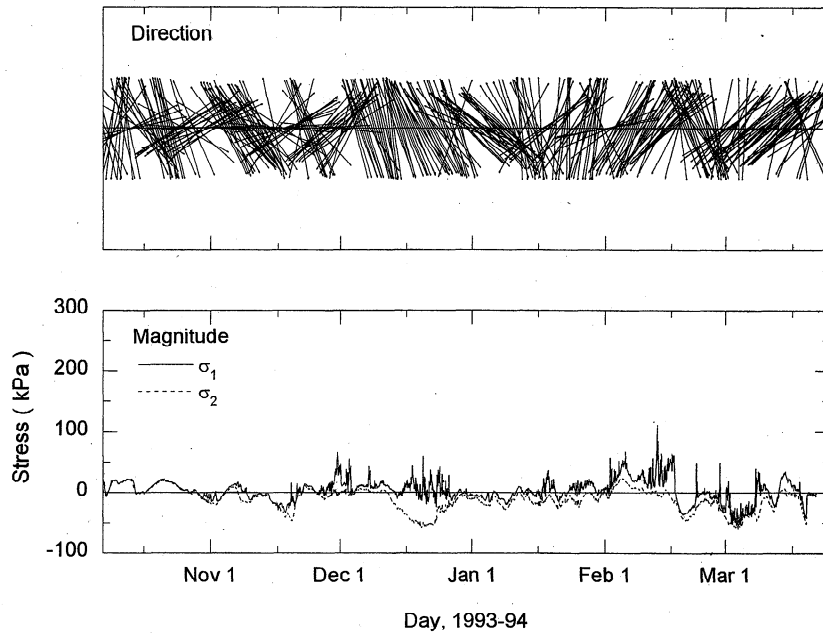


Figure 5a. Direction and magnitude of the major principal stress component at edge site 1 during the experiment. All angles are measured relative to the direction of the leg from edge site 3 to center site, which was originally oriented along true north (Figure 2).

Jones, 1993]. Using the stress time series from the Tucker and Perovich [1992] study and stress measurements made during the thermal loading of a first-year sea ice sheet [Lewis et al., 1994], Lewis [1995] suggests that the relatively small magnitude of the maximum tensile stress measured in the field may indicate the role that preexisting cracks play in reducing the overall strength of the ice. On the basis of a comprehensive set of fracture experiments on samples ranging in scale from 1 to 100 m, Dempsey [1996] suggests that there is a scale effect on the nominal tensile failure strength of Arctic sea ice. The relationship that he derives to explain this observed behavior

suggests that at a scale of 1 km the nominal tensile strength ranges from 11 to 38 kPa.

The spatial variability in stress between edge sites 1 and 3 was more pronounced than the variability within a given edge site. The linear regression analysis of the major principal stress at the 402-m edge site 3 and 2-m edge site 1 sensors over the entire experiment indicated a weak correlation of 0.58 (Table 2). The results of a similar analysis to establish the variation in σ_1 measured by the different sensors within each edge site are presented in Table 3. This analysis reveals a generally strong correlation between the sensor pairs at a given site. This is

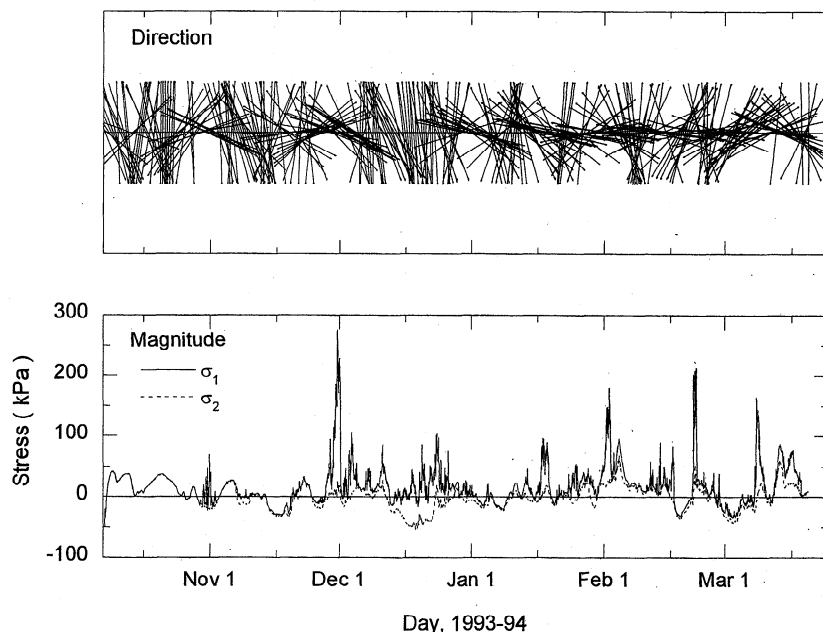


Figure 5b. Same as Figure 5a, but for edge site 3.

Table 2. Correlation Coefficients From a Linear Regression Analysis of Stress Measured by Sensors at Different Sites on the Floe

	Edge Site 1	Edge Site 3	Center Site
Edge Site 1, E1-2	1.00	0.80	0.74
Edge Site 3, E3-402	0.58	1.00	0.64
Center Site, C1-T	0.59	0.24	1.00

The lower triangle is the major principal stress, and the upper triangle is the minor principal stress.

most pronounced for sensor pairs 402 and 405C, 402 and 405L, and 402 and 410 at edge site 3 (Figure 2), where the correlation coefficient varies from 0.95 to 0.97. For sensor pair 402 and 425 at edge site 3, which is the farthest apart, the correlation coefficient decreases to 0.85. At edge site 1 the sensor pairs closest together again have the highest correlation coefficient. There was a poor correlation between the pair of sensors 2 and 75 m from the edge of the floe. The slope of the regression lines varied from 0.67 to 1.65, indicating that at these sites there was a small scale stress variation of $\pm 30\%$.

The correlation of stress between the sensor pairs at edge site 1 was typically lower than at edge site 3. This may be, in part, a function of the differences in the thickness distribution between the two sites. *Hallam et al.* [1989] and *Frederking and Evgin* [1990] have used models to show that under constant loading conditions the distribution of stress becomes more complex when the thickness distribution is nonuniform. Measurements by *Sukhorukov* [1995] support this result. It is apparent in Figure 3 that the ice thickness was more varied at edge site 1 than at edge site 3. The ice thicknesses measured over the extent of edge site 1 ranged from 0.54 to 2.11 m, with a mean and standard deviation of 1.21 ± 0.55 m. At edge site 3 the ice thickness ranged from 0.49 to 1.47 m, with a mean and standard deviation of 0.80 ± 0.29 m. Variations in the ice thickness may also explain why the changes in the correlation coefficient and the slope did not vary systematically as the distance between sensor pairs increased.

Combining our observations of the spatial variability between and within the sites on the multiyear floe, it is apparent that there was significant attenuation of the compressive stress as it was transmitted from the edge to the center of the floe. This attenuation did not occur rapidly over short distances near the edge of the floe. This differs from the results presented by *Perovich et al.* [1992], where the magnitude of the stress 15 m from the edge of a floe was only 24% of the stress measured 2 m from the edge. According to the finite element model results of *Frederking and Evgin* [1990], our observations of a less dramatic decrease in stress near the edge of the floe suggest that in this experiment, loads applied to the boundary of the floe were distributed over an area of several hundred meters. Using the range of peak stress measured at the edge sites, which was 50–200 kPa, and the average ice thickness of 1.44 m, the equivalent ridge-building force that would be distributed over this area is estimated to be 70–280 kN m^{-1} . This is consistent with the results of *Coon et al.* [1989], *Tucker and Perovich* [1992], and *Comfort et al.* [1994].

3.2. Thermal and Motion-Induced Stresses

Tucker and Perovich [1992] describe three sources of stress in the drifting pack ice in the eastern Arctic: changes in the ice temperature, ice motion due to winds and currents, and ice

motion due to tidal or inertial oscillations. In their measurements the ice-motion-induced stresses generated by tidal or inertial oscillations became evident as the floe moved into shallower waters and the pack began to break up. A power spectrum of the stress time series, presented by *Tucker and Perovich*, showed a strong peak at a period between 11.9 and 12.4 hours. A similar analysis of our data produced no such peak, indicating that under the conditions of this experiment there was no strong tidal or inertial source of stress. This is not surprising, given that the experiment took place over the winter when the ice pack has a high concentration and strength.

Thermal stresses are caused by the differential response of the ice to changes in the air temperature [*Evans and Untersteiner*, 1971; *Bogorodsky et al.*, 1972; *Lewis*, 1993]. Variations in the ice temperature due to changes in the air temperature first affect the top surface of the ice. The top of the ice cover attempts to expand or contract in response to the temperature change, but it is restricted by the lower portion of the ice which has yet to experience the thermal load. Stresses therefore develop through the thickness of the ice sheet, even though an actual change in ice temperature may only have penetrated the top portion of the ice cover.

Variations in the air temperature can occur rapidly and are often extreme. During this experiment, changes of 10°C to 20°C within a day were common (Figure 4d). The snow and ice cover act to damp these rapid variations, producing an in-ice variation of temperature that has a frequency of the order of days rather than hours. Evidence that these low-frequency changes in ice temperature produce a correspondingly low frequency stress is provided in Figure 4. It is apparent by visual comparison that the variations in the ice temperature record at center site are similar to the variations in the major principal stress at center site and the minor principal stress at all three sites.

Quantitative support of the relationship between ice stress and ice temperature was obtained by cross correlating these time series. In each cross correlation of ice temperature and stress we used the ice temperature measured by the thermistor mounted in the stress sensor. Before performing the correlation analysis, a 40-day high-pass filter was applied to the ice temperature and stress records to remove any long-term trends that might be generated by seasonal variations or instrument drift. The filter was designed and described by *Hibler* [1972]. An example to demonstrate the effectiveness of this filtering

Table 3. Results From a Linear Regression Analysis of the Stress Measured by Sensors Within an Edge Site

Sensor Pair	Horizontal Distance, m	Correlation Coefficient r	Slope	Intercept
<i>Edge Site 3</i>				
402:405C	3.0	0.95	1.11	11.46
402:405L	10.4	0.95	1.29	19.10
402:410	8.0	0.97	0.67	15.31
402:425	23.0	0.85	1.21	11.73
<i>Edge Site 1</i>				
2:5R	10.4	0.82	1.31	-23.44
2:10	8.0	0.88	1.65	8.05
2:75	73.0	0.49	1.04	23.40

In each case the regression line represents σ_1 (sensor at distance site, e.g., 405C) = slope [σ_1 (sensor 402)] + intercept. C, L, and R denote whether the sensor was along, to the left, or to the right, respectively, of the line running toward the center of the floe.

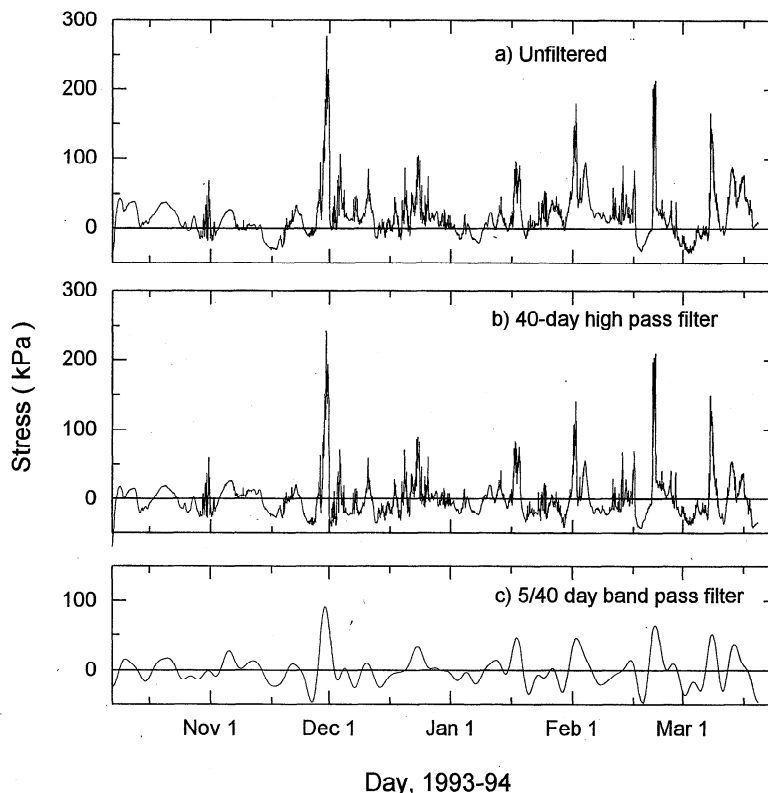


Figure 6. Time series of the major principal stress component at edge site 3 before and after applying a signal filter designed by *Hibler* [1972]: (a) unfiltered, (b) 40-day high-pass filter, and (c) 5-day/40-day band-pass filter.

technique is given in Figure 6, which shows the raw and filtered measurements for σ_1 at edge site 3. The results of the correlation analysis for the entire experiment (October 12 to March 7) are given in Table 4, where the peak correlation coefficient over a ± 10 -day window is given for each case. There is a consistently high correlation between ice temperature and the minor principal stress at all three sites, ranging from 0.86 to 0.80. The major principal stress is also strongly correlated with ice temperature at center site, with a peak correlation coefficient of 0.72. The correlation coefficient between the major principal stress and ice temperature is significantly weaker at the edge sites. The lowest correlation is at edge site 3, where the high-frequency content of the stress is most pronounced (Figure 4). In all cases the location of the peak correlation coefficient within the 20-day window indicated that the stress signal was leading the ice temperature. The average lead time

for these sensors, which were approximately 22 cm below the ice surface, was 0.6 ± 0.3 days, ranging from 0.0 to 1.2 days. This result demonstrates that stresses begin to develop at depth in the ice sheet as soon as a change in the ice temperature is felt at the top surface.

The characteristics of the time series at all the sites also indicate that the thermal stress measured at the sensor is isotropic in the plane of the ice sheet, which is consistent with observations made by *Tucker and Perovich* [1992] and *Prinsenberg et al.* [1997]. During periods of little high-frequency activity, when we assume that the thermal stresses are dominant, the major and minor principal stresses are typically approximately equal, for example, October 12–29, November 4–26, and January 5–11 (Figure 4). Deviations in the magnitude of the major and minor stress components increase as the high-frequency content in the major principal stress signal increases.

Table 4. Peak Correlation Coefficients From a ± 10 -Day Cross-Correlation Analysis of the Major σ_1 and Minor σ_2 Principal Stress Components and Ice Temperature

Correlation Period	Filter Type	Edge Site 3		Edge Site 1		Center Site	
		σ_1	σ_2	σ_1	σ_2	σ_1	σ_2
Oct. 12 to March 7	40-day high pass	0.30	0.84	0.43	0.86	0.72	0.80
	2-day/40-day band pass	0.33		0.48			
	5-day/40-day band pass	0.37		0.53			
Oct. 12 to Nov. 26	40-day high pass	0.68	0.89	0.78	0.91	0.62	0.75
Nov. 26 to March 7	40-day high pass	0.23	0.85	0.35	0.85	0.83	0.85

A filter [Hibler, 1972] was applied to all time series before performing the cross correlation. The wavelength of the filter used on the stress time series is indicated for each case.

This is particularly evident from December 8 to January 2. As we demonstrated earlier, the stress exhibits strong directionality during these periods of high-frequency activity.

The most significant thermal event during the winter occurred around February 4, when the air temperature rose from -36°C to -3°C in 2 days (Figure 4d). This caused an increase in ice temperature at a depth of 22 cm of approximately 5°C . Correspondingly, there was a 75 to 100 kPa increase in the compressive stress at all three sites. More typically, variations in air temperature during the winter were 10°C to 20°C , causing changes in the ice temperature of $1\text{--}3^{\circ}\text{C}$ and stress variations of 25 to 50 kPa. In all cases, each 1°C change in the ice temperature created a change in stress of 15–20 kPa. This is the same order of magnitude effect reported by *Tucker and Perovich* [1992], who observed a 125-kPa increase in stress with a 2.5°C increase in ice temperature at a sensor 25 cm below the ice surface of a 2-m-thick multiyear ice floe. *Johnson et al.* [1985] measured a 500-kPa increase in stress associated with an 8°C increase in ice temperature at a depth of 0.49 cm in a 1.7-m-thick first-year ice sheet that was adjacent to a caisson-retained island. *Sukhorukov* [1995] reported that near the surface of a multiyear floe a 1°C change in temperature caused a 50-kPa variation in ice stress. *Prinsenberg et al.* [1997] found the temperature effects near the top of a landfast coastal sea ice sheet to be $1\text{ kPa }^{\circ}\text{C}^{-1}$, an order of magnitude lower than the other combined results suggest. This difference may be a function of the ice environment and stress sensor type. Our stress measurements and those reported by *Tucker and Perovich* [1992] and *Johnson et al.* [1985] were all made using the same type of stress sensor, while *Prinsenberg et al.* [1997] used rosettes of mercury-filled disk diaphragms.

Ice-motion-induced stresses occur in response to wind and current forcing and can result in the formation of ridges, leads, and rubble fields. Observations of stress and ice deformation have shown that these ice deformation events are associated with large and rapid changes in the ice stress [*Johnson et al.*, 1985; *Coon et al.*, 1989; *Comfort et al.*, 1992; *Tucker and Perovich*, 1992]. We made similar observations during this experiment. In two cases, November 29 and February 17, visual inspections of the floe before and after these events indicate that rapid decreases in stress were associated with cracks and, subsequently, leads forming across the multiyear floe. No one was on the floe to make similar observations during other periods of significant stress activity.

To further develop the understanding of pack ice rheology using in situ stress measurements like those presented in this paper, it is necessary to separate out the motion-induced stresses. A rheology specifically relates deformation to the stresses caused by that deformation. Given that thermal stresses produce a dominantly low frequency signal and that the distinguishing characteristic of the ice-motion-induced stresses is the rapid variation in magnitude, we explored the use of signal-filtering techniques to separate the different stresses. Specifically, we applied a 2-day/40-day and 5-day/40-day band-pass filter to the stress data in an attempt to isolate the thermal stress signal. The stress time series at edge site 3 after the 5-day/40-day band-pass filter was applied is given in Figure 6. Low-frequency peaks in the stress are still apparent, while the high-frequency variations have been removed. To assess the effectiveness of this technique, we performed a cross-correlation analysis of the processed stress and ice temperature for the major principal stress component at the edge sites. As seen in Table 4, there was only a slight improvement

in the correlation coefficient when the period chosen for the correlation ran over the entire length of the experiment. At edge site 1, for a 5-day/40-day band-pass filter, the correlation increased from 0.43 to 0.53, and at edge site 3 it increased from 0.30 to 0.37. This result indicates that the source of the low-frequency content in the stress signal at the edge site is not strongly associated with the thermal loading. It further implies that while the high-frequency content in the ice-motion-induced stress signal is a distinguishing characteristic, there is also a significant low-frequency content. One possible explanation for this observation is that the pack essentially undergoes strain hardening during an ice motion event. When enough momentum is generated for the pack to begin to converge, compressive stresses begin to build. With continued loading and convergence, the stress increases until areas of relatively thin ice in the region begin to fail. These local failures cause a rapid decrease in the stress signal but not a total loss of strength. Instead, by removing areas of weakness, the failure of the thin ice acts to strengthen the pack and the compressive stress can continue to slowly build. This process creates a stress signature that exhibits rapid fluctuations overlying a gradual increase in stress. It continues until the event generating the momentum ends and stresses gradually decrease or until the compressive stresses build to the point that the thick multiyear floes fail and large lead systems develop.

The consistently strong correlation between the ice temperature and the minor principal stress offers another approach for separating the thermal and ice-motion-induced stresses. If the minor principal stress is primarily a function of changes in the ice temperature and thermal stresses are isotropic in the plane of the ice cover, then the ice-motion-induced stresses can be estimated by subtracting the minor from the major stress. This approach was applied at the edge and center sites, and the results are presented in Figure 7. No filters were applied to the data for this part of our analysis. At all sites the most pronounced characteristic of the estimated ice-motion-induced stress is the absence of tensile stresses. This is an artifact of the technique we have applied since, by definition, $\sigma_2 \leq \sigma_1$. Under certain loading conditions, ice-motion-induced stresses may, in fact, be predominantly compressive. However, even in these cases, irregularities in the thickness of the multiyear floe are likely to cause bending, which can result in tensile stresses [*Hallam et al.*, 1989; *Frederking and Evgin*, 1990; *Sukhorukov*, 1995]. The estimated ice-motion-induced stress exhibits both high- and low-frequency variations at all of the sites. There are no significant changes in the relative magnitude of the peak stresses nor in the relative distribution between the sites for the estimated ice-motion-induced stress. Edge site 3 still shows more pronounced high-frequency activity than edge site 1, and center site remains dominated by low-frequency variations. The existence of periods of approximately zero stress, which occur between the episodes of high-frequency activity at the edge sites, is intuitively pleasing. These periods of near-zero stress were not present at center site between November 27 and February 20. Instead, the estimated ice-motion-induced stress at center site is more persistent, varies at a low frequency, and consistently exhibits a maximum of approximately 40 kPa. The difference between characteristics of the estimated ice-motion-induced stress between the edge and center sites may reflect the complex process of stress transmission through floe and, more generally, the ice pack.

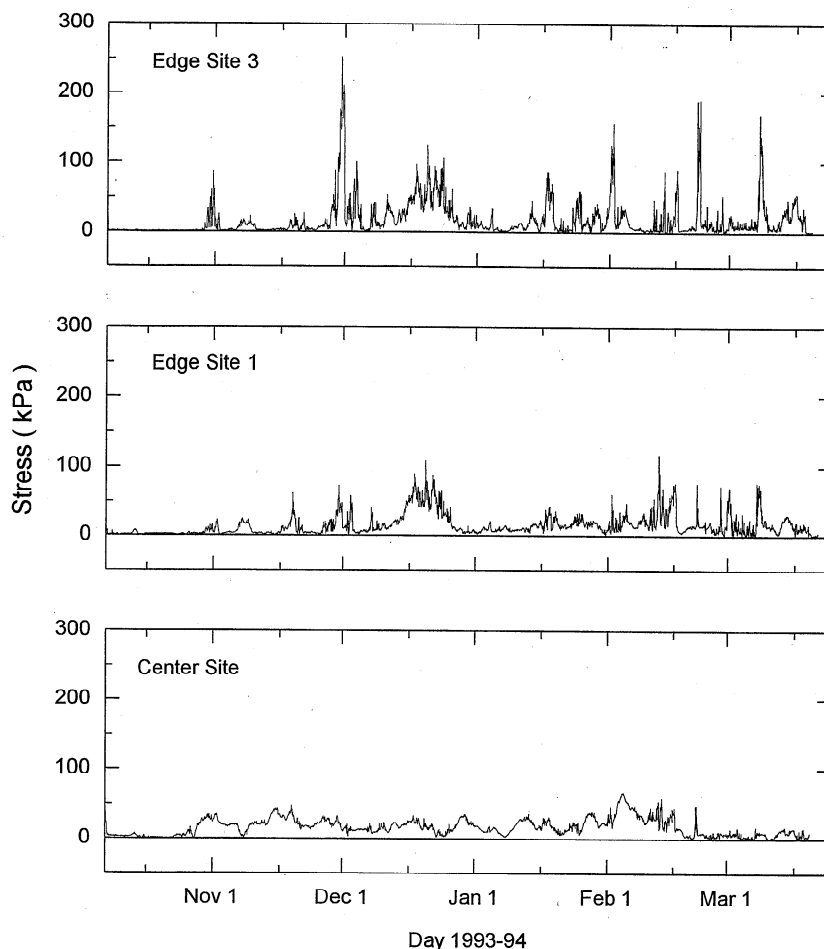


Figure 7. Estimated ice-motion-induced stresses obtained by subtracting the minor from the major principal stress component.

3.3. Seasonal Dependence

A subtle seasonal change in the characteristics of ice pack behavior is apparent in the stress time history of the major principal stress at the edge sites (Figure 4). Before November 26, variations in the stress signal are predominantly low in frequency, with an isolated high-frequency event occurring from October 30 to November 3. After November 26 the high-frequency content of the stress signal becomes more persistent, with a few isolated periods of low-frequency activity. The cross-correlation analysis of stress and ice temperature, using a 40-day high-pass filter, was repeated for the periods October 12 to November 26 and November 26 to March 7, and the results are given in Table 4. Comparing the peak correlation coefficients for these periods with those obtained when considering the stress over the entire experiment confirms quantitatively a change in the characteristic of stress. There is a significant and consistent improvement in the correlation of stress and ice temperature for the major principal component at the edge sites for October 12 to November 26 period. The peak correlation coefficients increase to 0.68 and 0.78 for edge sites 1 and 3, respectively. There is little change in the correlation coefficients between these periods of consideration for the minor principal stress components at the edge sites and for either stress component at center site. These results suggest that in the fall and early winter the stresses throughout the floe have

a strong thermal content. As the winter proceeds, the relationship between stress and ice temperature at the edges of the floe becomes less apparent as the ice-motion-induced stresses become persistent. The seasonal variation is also apparent in the times series of the estimated ice-motion-induced stress (Figure 7), where stress at the edge sites is approximately 0 kPa for most of this period.

We believe that this result reflects the effect that ice thickness and rigidity have on the continuum behavior of the ice cover under conditions of high ice concentration. During fall freeze-up, when the ice between the isolated multiyear floes initially forms, it is thin and soft and cannot effectively transmit stresses that develop in the pack. Only local failure events around the boundary of the floe create ice-motion-induced stresses in the floe. As the ice between the floes begins to thicken and becomes more rigid, the pack behaves more like a mechanical continuum, with failures in the pack creating a more dispersed stress field. Stresses measured in the floe are often associated with ice failure in other parts of the ice pack. This hypothesis is consistent with the assumptions made in the development of ice dynamics models [Thorndike *et al.*, 1975; Hibler, 1979]. In these models, pack ice strength is represented as a function of the amount of thin ice and its thickness. The ice strength increases as the amount of thin ice is reduced owing, in part, to thickening by thermodynamic growth.

4. Conclusions and Suggestions for Future Work

Our analysis of a 6-month-long time series of stress near the edge and at the center of a multiyear floe indicates that during this winter experiment there were two types of stress: thermal and ice motion induced. Changes in the ice temperature, caused by changes in the air temperature, generate both tensile and compressive stresses that vary slowly, at a frequency of the order of days. The magnitude of the thermal stresses is relatively constant at a given depth over the extent of a multiyear floe. Variations in the ice temperature are strongly correlated with the minor principal stress component. This result suggests that the minor principal stress component provides a good first-order approximation of the thermally induced stresses in the floe. It also provides a simple technique for obtaining an approximate representation of the ice-motion-induced stress for the direct evaluation of pack ice rheology: subtracting the minor from the major principal stress component.

Ice-motion-induced stresses, which in the winter are primarily caused by atmospheric forcing, exhibit significant spatial variability over the extent of a floe. At the edges of a floe, ice-motion-induced stresses are most easily distinguished by rapid variations in magnitude, which occur at a frequency of the order of hours. These stresses also appear to have a significant low-frequency content similar to the thermally induced stresses. This makes it difficult to use signal-filtering techniques to separate the thermal and ice-motion-induced stresses. The observation of rapid changes in the stress magnitude, superimposed on lower-frequency variations, implies that the pack undergoes strain hardening as it converges. Areas of relatively thin ice fail and effectively increase the overall strength of the ice cover for the duration of the convergence event.

The magnitude of the combined thermal and ice-motion-induced stresses displays significant temporal and spatial variability in compression. Maximum compressive stresses, measured at a site 400 m from the edge of the floe, typically ranged from 100 to 200 kPa and suggest a ridge-building force of the order of 150 kN m^{-1} . These stresses are significantly attenuated as they are transmitted from the edge to the center of the floe. Tensile stresses are much more consistent over the entire floe, reaching a maximum of 50 kPa. The relative magnitude of the stress between sites at the edge of the floe, the direction of the principal stress, and a correspondence in the time of occurrence of episodes of significant stress activity between the sites remained fairly constant during the experiment. This implies that the loading and boundary conditions that generated the observed distribution of stress remained relatively consistent through the winter season during this experiment.

There are seasonal changes in the characteristics of the total stress. Thermally induced stresses are dominant in the fall. Ice-motion-induced stresses become more persistent as the winter season progresses. This suggests that the ice cover cannot effectively transmit stresses through the pack until the new ice that develops in the fall between the multiyear floes becomes thick and rigid enough to create a mechanical continuum.

Together, these results demonstrate the complex process of stress transmission specifically through a multiyear floe and more generally through the ice pack. Following the lead of *Frederking and Evgin* [1990], a more detailed understanding of the process of stress transmission through the floe can be developed. A finite element model can be used to estimate the

boundary conditions that produced the stress distribution in the floe. The pack ice rheology assumed in ice dynamics models can be evaluated and further developed by coupling the stress measurements with concurrent measurements of ice deformation made during this experiment [*Richter-Menge et al.*, 1996]. This includes both continuum [*Hibler*, 1979] and granular-based [*Hopkins*, 1996] models. The assumed rheology can be evaluated by driving the models with the environmental loading conditions that existed during this experiment. Once general agreement of the modeled and observed ice motion is achieved, the ice stresses required for the model run can be determined and compared to the measured stresses. If the modeled and measured ice stresses do not agree, then the model assumptions can be reevaluated and modified and the process repeated. An effort like this would provide a direct, rather than implicit, technique for assessing the internal ice stress term in the momentum balance equation, which is central to large-scale ice dynamics models.

Acknowledgments. We extend our thanks for the tremendous field support provided by the logistics team from Polar Science Center, University of Washington, which was led by Andy Heiberg and included Jay Ardaï from Lamont-Doherty Earth Observatory. The analysis and interpretation of our results have greatly benefited from discussion with Mark Hopkins, Jim Overland, Don Perovich, and Terry Tucker. Support for this work was provided by the Office of Naval Research and the Cold Regions Research and Engineering Laboratory.

References

- Bogorodsky, V. V., V. P. Gavrilov, A. V. Gusev, Z. M. Gudkovich, and A. P. Polyakov, Stressed ice cover state due to thermal wave and related underwater noise in the ocean (in Russian), paper presented at Ice Symposium, Int. Assoc. for Hydraul. Res., Leningrad, 1972. (English translation, IAHR, pp. 28–33, 1972.)
- Comfort, G., and R. Ritch, Field measurements of pack ice stress, in *Proceedings of the Ninth International Conference on Offshore Mechanics and Arctic Engineering*, vol. 4, *Arctic/Polar Technology*, edited by O. A. Ayorinde, N. K. Sinha, and D. S. Sodhi, pp. 177–181, Am. Soc. of Mech. Eng., New York, 1990.
- Comfort, G., R. Ritch, and R. M. W. Frederking, Pack ice stress measurements, in *Proceedings of the Eleventh International Conference on Offshore Mechanics and Arctic Engineering*, vol. 4, edited by O. A. Ayorinde, et al., pp. 245–253, Am. Soc. of Mech. Eng., New York, 1992.
- Comfort, G., A. Dinnovitzer, and Y. Gong, Limit-force ice loads and their significance to offshore structures in the Beaufort Sea. *Rep. 4346-C*, Fleet Technol. Ltd., Kanata, Ont., 1994.
- Coon, M. D., P. A. Lau, S. H. Bailey, and B. J. Taylor, Observations of ice floe stress in the eastern Arctic, in *Proceedings of the 10th International Conference on Port and Ocean Engineering Under Arctic Conditions*, vol. 1, edited by K. B. E. Axelsson and L. A. Fransson, pp. 44–53, Lulea Univ. of Technol., Lulea, Sweden, 1989.
- Cox, G. F. N., and J. B. Johnson, Stress measurements in ice, *Rep. 83-23*, Cold Reg. Res. and Eng. Lab., Hanover, N. H., 1983.
- Croasdale, K. R., G. Comfort, R. M. W. Frederking, B. W. Graham, and E. L. Lewis, A pilot experiment to measure Arctic pack ice driving forces, in *Port and Ocean Engineering Under Arctic Conditions*, vol. 3, edited by W. M. Sackinger and M. O. Jeffries, pp. 381–395, Geophys. Inst. Univ. of Alaska, Fairbanks, 1988.
- Dempsey, J. P., Scale effects in the fracture of sea ice, in *The Johannes Weertman Symposium*, edited by R. J. Arsenault, et al., pp. 351–362, Miner., Metals, and Mater. Soc., Warrendale, Pa., 1996.
- Dykens, J. E., Ice engineering: Tensile properties of sea ice grown in a confined system, *Tech. Rep. R680*, Nav. Civil Eng. Lab., Port Hueneme, Calif., 1970.
- Evans, R. J., and N. Untersteiner, Thermal cracks in floating ice sheets, *J. Geophys. Res.*, 76(3), 694–703, 1971.
- Frederking, R. M. W., and E. Evgin, Analysis of stress distribution in an ice floe, in *Proceedings of the Ninth International Conference on*

- Offshore Mechanics and Arctic Engineering*, vol. 4, *Arctic/Polar Technology*, edited by O. A. Ayorinde, N. K. Sinha, and D. S. Sodhi, pp. 83–87, Am. Soc. of Mech. Eng., New York, 1990.
- Hallam, S. D., N. Jones, and M. W. Howard, The effect of sub-surface irregularities on the strength of multi-year ice, *ASME J. Offshore Mech. Arc. Eng.*, *111*, 350–353, 1989.
- Hibler, W. D., III, Design and maximum error estimation for small error low pass filters, *Res. Rep. 304*, Cold Reg. Res. and Eng. Lab., Hanover, N. H., 1972.
- Hibler, W. D., III, A dynamic thermodynamic sea ice model, *J. Phys. Oceanogr.*, *9*, 815–846, 1979.
- Hibler, W. D., III, Modeling a variable thickness sea ice cover, *Mon. Weather Rev.*, *108*(12), 1943–1973, 1980.
- Hopkins, M. A., On the mesoscale interaction of lead ice and floes, *J. Geophys. Res.*, *101*(C8), 18,315–18,326, 1996.
- Johnson, J. B., and G. F. N. Cox, Stress sensor particularly suited for elastic, plastic, and viscoelastic materials, U. S. patent 4,346,600, August 31, 1982.
- Johnson, J. B., G. F. N. Cox, and W. B. Tucker, Kadluk ice stress measurement program, in *8th International Conference on Port and Ocean Engineering Under Arctic Conditions*, Dan. Hydraul. Inst., Horsholm, Denmark, 1985.
- Kuehn, G. A., R. W. Lee, W. A. Nixon, and E. M. Schulson, The structure and tensile behavior of first-year sea ice and laboratory-grown saline ice, *ASME J. Offshore Mech. Arc. Eng.*, *112*, 357–363, 1990.
- Lewis, J. K., A model for thermally-induced stresses in multi-year sea ice, *Cold Reg. Sci. Technol.*, *21*, 337–348, 1993.
- Lewis, J. K., A conceptual model of the impact of flaws on the stress state of sea ice, *J. Geophys. Res.*, *100*(C5), 8829–8835, 1995.
- Lewis, J. K., W. B. Tucker III, and P. J. Stein, Observations and modeling of thermally induced stresses in first-year sea ice, *J. Geophys. Res.*, *99*(C8), 16,361–16,371, 1994.
- Nikitin, V. A., and S. A. Kolesov, Stresses and forces under ice compacting, *Int. J. Offshore Polar Eng.*, *3*(2), 139–142, 1993.
- Oberhuber, J. M., Simulation of the Atlantic circulation with a coupled sea ice-mixed layer-isopycnal general circulation model, I, Model description, *J. Phys. Oceanogr.*, *23*, 808–829, 1993.
- Perovich, D. K., K. F. Jones, and W. B. Tucker III, Observations of stress in Arctic pack ice, paper presented at 11th International Symposium on Ice, Int. Assoc. for Hydraulic Res., Banff, Alberta, Canada, June 15–19, 1992.
- Perovich, D. K., B. C. Elder, and J. A. Richter-Menge, Observations of the annual cycle of sea ice temperature and mass balance, *Geophys. Res. Lett.*, *24*(5), 555–558, 1997.
- Pollard, D., and S. L. Thompson, Sea ice dynamics and CO₂ sensitivity in a global climate model, *Atmos. Ocean*, *32*(2), 449–467, 1994.
- Prinsenber, S. J., G. A. Fowler, A. van der Baaren, and B. Beanlands, Ice stress measurements from land-fast ice along Canada's Labrador coast, *Cold Reg. Sci. Technol.*, *25*, 1–16, 1997.
- Richter-Menge, J. A., and K. F. Jones, The tensile strength of first-year sea ice, *J. Glaciol.*, *39*(133), 609–618, 1993.
- Richter-Menge, J. A., B. C. Elder, J. E. Overland, and S. Salo, Relating Arctic pack ice stress and strain at the 10km scale, in *Proceedings of the ACSYS Conference on the Dynamics of the Arctic Climate System*, edited by P. Lemke, et al., *WMO/TD Publ. 760*, pp. 327–331, World Meteorol. Organ., Geneva, 1996.
- Rothrock, D. A., The energetics of the plastic deformation of pack ice by ridging, *J. Geophys. Res.*, *80*(33), 4514–4519, 1975.
- Semtner, A. J., A numerical study of sea ice and ocean circulation in the Arctic, *J. Phys. Oceanogr.*, *17*, 1077–1099, 1987.
- Sukhorukov, K. K., Internal stresses at typical local inhomogeneities of sea ice cover, paper presented at 13th International Conference on Port and Ocean Engineering Under Arctic Conditions, Am. Soc. of Mech. Eng., Murmansk, Russia, Aug. 15–18, 1995.
- Thorndike, A. S., D. A. Rothrock, G. A. Maykut, and R. Colony, The thickness distribution of sea ice, *J. Geophys. Res.*, *80*(33), 4501–4513, 1975.
- Tucker, W. B., III, and D. K. Perovich, Stress measurements in drifting pack ice, *Cold Reg. Sci. Technol.*, *20*, 119–139, 1992.
- Weatherly, J. W., T. W. Bettge, and W. M. Washington, Simulation of sea ice in the NCAR climate model system, *Ann. Glaciol.*, *25*, 107–110, 1997.

B. C. Elder and J. A. Richter-Menge, Cold Regions Research and Engineering Laboratory, 72 Lyme Road, Hanover, NH 03755. (e-mail: jr RichterMenge@crrel.usace.army.mil)

(Received March 19, 1997; revised October 2, 1997; accepted January 7, 1998.)